A Study on Electric Vehicle Battery Ageing Through Smart Charge and Vehicle-to-Grid Operation

Truong Minh Ngoc Bui
Energy Innovation Centre, WMG
University of Warwick
Coventry, United Kingdom
truong.bui@warwick.ac.uk

Truong Quang Dinh
Energy Innovation Centre, WMG
University of Warwick
Coventry, United Kingdom
t.dinh@warwick.ac.uk

James Marco
Energy Innovation Centre, WMG
University of Warwick
Coventry, United Kingdom
james.marco@warwick.ac.uk

***Abstract*— Electrification of transportation means brings positive impacts to the environment because of reduced fossil fuel depletion and related carbon emissions. Critical obstacles remain in terms of battery costs and their expected life. Vehicle-to-grid technologies can deliver benefits to support electrical power grid and vehicle owner, while their practical implementation faces challenges due to the concerns over accelerated battery degradation. This study presents the evaluation of battery degradation through different smart charge strategies and vehicle-to-grid scenarios. The simulation results show that the developed smart charge schemes can mitigate the battery ageing up to 5% while lowering the charge cost from 30 – 60% as comparing to the conventional charge method within the first five days operation of the battery. In addition, the calendar ageing can be diminished upto 80% by participating in suitable V2G scenario.**

Keywords—vehicle-to-grid, battery ageing, smart charge, calendar ageing, cycling ageing

I. INTRODUCTION

The market infiltration of electric vehicles (EVs), which demonstrates a small segment of the entire global automotive industry, is significantly expanding due to their considerable benefits in dealing with environmental concerns. Vehicle-to-grid (V2G) technologies, which allow the battery of the EV to be connected to the electrical power grid to provide extra energy and support ancillary services such as frequency regulation, peak load shaving balancing, becomes increasingly crucial, especially where conventional forms of energy storage are unavailable or costly [1-4]. In V2G operations, the batteries are not only charged, but also can act as mobile energy storage systems to return energy back to the grid when the vehicle is parked and remains connected. A critical challenge obstructing the implementation of V2G is the concerns over battery degradation. Literature shows several research presenting different approaches and methodologies to deal with battery degradation when participating in V2G scenarios [5-8]. However, most of the studies evaluated either calendar ageing or cycling ageing under stable operational conditions. A few studies attempted to combine both ageing mechanisms into a single ageing model to evaluate the holistic battery degradation behavior but were not evaluated under real-world operation.

This study presents the evaluation of battery degradation through different smart charge strategies and vehicle-to-grid scenarios. A semi-empirical degradation approach is employed to model the battery ageing behaviour with respect to calendar and cycling ageing. Then, a synthesized degradation model is developed to fully demonstrate the ageing of the battery under different operational condition. Then, three charging strategies are proposed to underpin the evaluation of battery degradation under two V2G scenarios. The remainder of the paper includes: the development of battery degradation model is discussed in section II. Section III presents the case studies, which consist of the development of charging strategies and V2G scenarios. Section IV shows the simulation results and discussion. Conclusion and future works are finalized in section V.

II. BATTERY AGEING DEVELOPMENT

The rate of battery degradation is often governed by how the battery is used and stored. It is generally indicated by the so-called ageing stress factors including temperature, SoC, time, charge throughput, DoD and C-rate. The battery capacity fade can be categorized into two groups namely calendar ageing and cycling ageing, which are dependent on different ageing stress factors. Calendar ageing represents the capacity loss of the battery at idle state when there is no external loaded, while the cycling ageing depicts the capacity fade of the battery at operational state where there is an amount of charge passing through.

A. Battery Selection

To estimate the evolution of the capacity fade and support model parameter identification and verification, Lithium-ion Nickel Manganese Cobalt ($Ni_xMn_yCo_{1-x-y}$) oxide cathode and LiC_6 (graphite) anode cylindrical cells are utilised for long-term ageing test with different conditions. The cell model name is INR21700 M50 manufactured by LG Chem with a 3.63V of nominal voltage and rated capacity at 5.00Ah. The lower and upper cut-off voltages are 2.5V and 4.2V, respectively as recommended by the manufacturer. Before conducting the tests, all cells are pre-conditioned allowing their materials stabilisation and removing the remaining electrochemical interactions within the cells caused by the manufacturing process. Then, the cells are characterised for initial parameterisation purposes following the procedures described in our previous works [9, 10]. Therefore, at the beginning of the ageing tests, the cell characteristic is captured and the initial SoH is set to be 100%.

B. *Battery Ageing Modelling*

Several studies have developed different strategies to represent the battery degradation behaviours such as empirical, semi-empirical, electrochemical-based, data-driven-based and machine learning approaches [2, 11, 12]. Each approach has their specific advantages and disadvantages. However, since the purpose of the battery degradation modelling in this study is to evaluate ageing behaviours under different charging strategies and V2G scenarios, simple degradation models that satisfy the model accuracy and computational effort are deemed to be adequate. It is because the underpinning degradation mechanisms requiring high-fidelity models are not necessary in this case. Instead, a model with fast execution rate is enough to simulate long-term degradation behaviour of the battery in the scale of months and years of operational life. Hence, the semi-empirical modelling approach is selected for this study.

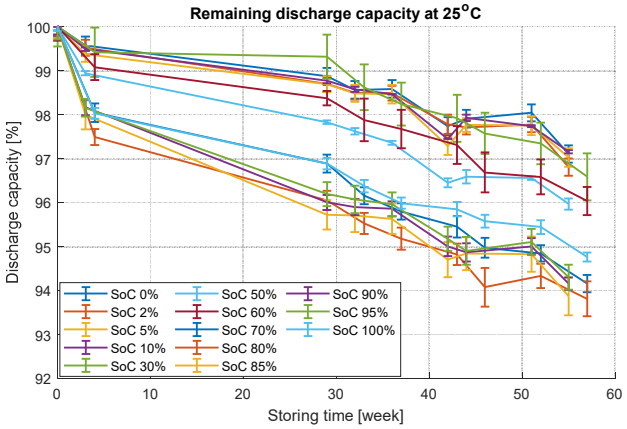

Fig. 1. Capacity measurement of the calendar ageing test

To support the model development, two batches of the selected battery are used for the calendar and cycling ageing study tests separately. Firstly, a batch of 39 cells is being employed for calendar ageing tests. These cells are stored at 25^0C at 13 different SoCs from 0 – 100%. The set of data of the calendar ageing tests selected in this study ends at 57 weeks while the ageing process is still ongoing until reaching the battery's end-of-life (EoL). Fig. 1 shows the discharge capacity measurements during the test. Basically, the cells' capacity measurement is taken place every two weeks during the test. However, due to the laboratory access limitation recently, the capacity snapshots are carried out irregularly as shown in Fig. 1.

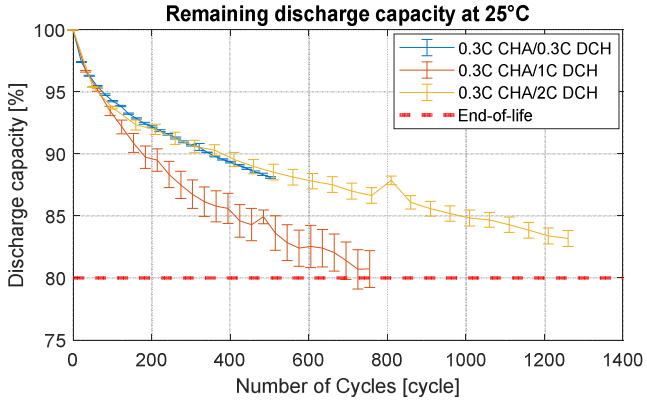

Fig. 2. Capacity measurement of the cycling ageing test

Secondly, another batch consists of 9 cells is being used for cycling ageing test. The tests are carried out at one charge C-rate and three different discharge C-rates, which are 0.3, 1.0 and 2.0 C, at ambient temperature of 25^0C. The cells are fully charged and discharged repeatedly without any interruption. The set of data using in this study is depicted in Fig. 2 while the tests are currently ongoing until reaching the battery's EoL, where the capacity drops to below 80%. During the test, the discharge capacity measurements are performed every two weeks.

1) *Calendar Capacity Loss*

The capacity loss due to calendar ageing is described as a function of temperature, battery SoC and time. The semi-empirical model can be given as follows:

$$Q_{loss}^{cal} = \lambda_{tmp}.\lambda_{SoC}.\tau^{\gamma_{cal}} \quad (1)$$

where, λ_{tmp} and λ_{SoC} are the calendar temperature and SoC coefficient, respectively; τ is the storing duration, γ_{cal} is a calendar exponential factor ($\gamma_{cal} = 0.5$).

The temperature coefficient represents the effect of temperature to the calendar ageing at different SoC at the operational temperature. It can be described via the Arrhenius law as follows:

$$\lambda_{tmp} = \lambda_R.\exp\left(-\frac{\varepsilon}{R}\left(\frac{1}{T}-\frac{1}{T_R}\right)\right) \quad (2)$$

where, ε is the activation energy, R is the gas constant, T and T_R are the testing temperature and reference temperatures, λ_R is a reference constant.

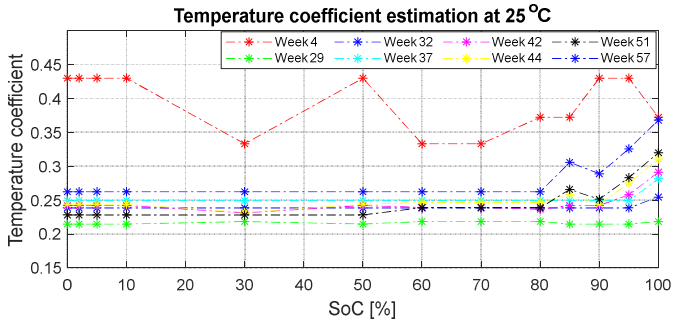

Fig. 3. Temperature coefficient at different SoC

The SoC coefficient, which illustrates the influence of storing SoC to the calendar ageing at different time and temperatures, can be expressed as below:

$$\lambda_{SoC} = \beta_1 SoC^3 + \beta_2 SoC^2 + \beta_3 SoC + \beta_4 \quad (3)$$

where, β_1, β_2, β_3, β_4 are the SoC fitting constants of the polynomial, which are estimated using curve fitting method.

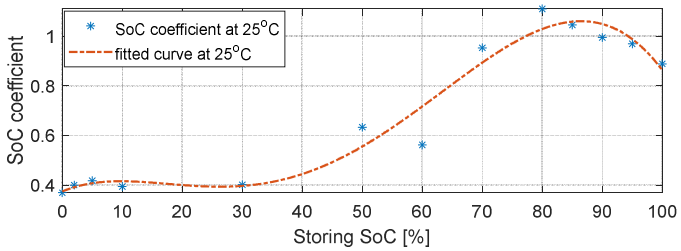

Fig. 4. SoC coefficient curves

Fig. 3 and 4 show the estimated temperature and SoC coefficients with respect to different SoC, respectively. From these figures, at any instant of SoC, we can interpolate a temperature and SoC coefficient accordingly.

2) *Cycling Capacity Loss*

The capacity loss due to cycling ageing can be expressed as a function of DoD, C-rate and Ah throughput. The semi-empirical ageing model can be described as follows:

$$Q_{loss}^{cyc} = \lambda_{Crate}.\lambda_{DoD}.\lambda_{Ah}^{\gamma_{cyc}} \tag{4}$$

where, λ_{Crate} and λ_{DoD} are the C-rate and DoD coefficient, respectively, λ_{Ah} is the Ah throughput, γ_{cyc} is the cycling exponential factor (γ_{cyc} = 0.5).

The Ah throughput depicts the amount of charge delivered by the battery during cycling and can be calculated as the multiplication of DoD, number of full charge cycle and battery capacity. It can be expressed as follows:

$$\lambda_{Ah} = DoD.N_E.C_P \tag{5}$$

where, N_E is the number of equivalent full charge cycle, C_P is the battery capacity.

The C-rate coefficient presents the influence of the charge C-rate to the battery capacity fade during cycling. It can be estimated based on the historical ageing data though the following term:

$$\lambda_{Crate} = \frac{Q_{loss}^{*}}{\left(\lambda_{Ah}^{*}\right)^{\gamma_{cyc}}} \tag{6}$$

where, Q_{loss}^{*} and λ_{Ah}^{*} are the measured capacity loss and Ah throughput due to cycling ageing, respectively.

To solely estimate the C-rate coefficient, historical ageing data at a reference point, which is at 100% DoD, is employed. At this point, it is supposed that the effect of DoD to the battery capacity fade is unchanged and can be set equivalent to one when calculating the C-rate coefficient.

The DoD coefficient represents the effect of the discharge depth to the battery ageing during cycling and can be calculated based on the substitution of (5), (6) into (4), forming (7).

$$\lambda_{DoD} = \frac{Q_{loss}^{*}}{\lambda_{Crate}^{*}\left(\lambda_{Ah}^{*}\right)^{\gamma_{cyc}}} \tag{7}$$

where, λ_{Crate}^{*} is the C-rate coefficient at the reference point.

3) *Synthesized Degradation Model*

The continuous capacity loss in functions (1) and (4) can be used to estimate the capacity degradation of the battery under a fixed operational condition, for example, under resting/storing states or operating states. However, to estimate the complete battery ageing under a mixed of working condition such as a real-world driving profile, which including driving and resting periods, a synthesized degradation is considered by updating the combined calendar and cycling ageing function incrementally. Hence, the total capacity loss can be predicted by the sum of calendar capacity loss (when the battery is in idle state) and cycling capacity loss (when the battery is in operational state).

$$\begin{aligned} Q_{loss}^{total} &= Q_{loss}^{cal} + Q_{loss}^{cyc} \\ &= \lambda_{tmp}.\lambda_{SoC}.\tau^{\gamma_{cal}} + \lambda_{Crate}.\lambda_{DoD}.\lambda_{Ah}^{\gamma_{cyc}} \end{aligned} \tag{8}$$

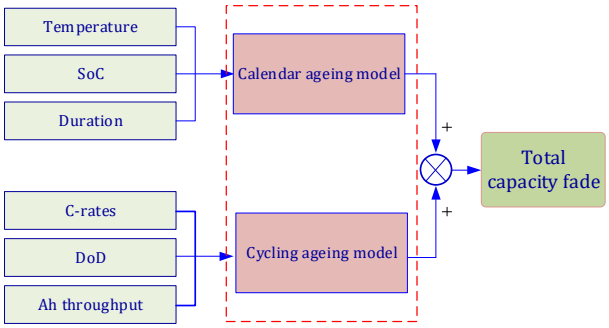

Fig. 5. Synthesized degradation model framework

Fig. 5 shows schematically the synthesized degradation model framework. The total capacity fade can be estimated based on the combination of calendar and cycling ageing accordingly. This combination was considered and evaluated as the generic approach for predicting the complete battery ageing under mixed driving cycles in the literature [13, 14]. At any instantaneous of time, either calendar or cycling ageing is considered as the main contribution to the total capacity loss.

III. Case Study Development

A. *Operational Profiles*

A five-day operational profile is introduced using real-world driving data of EV driving trials. The profile consists of ten individual driving trips in combining with customised parking, charging cycles in between. To simulate a complete daily operation of an EV, each day includes two driving cycles (drive-to-work and drive-to-home) interspersed with two parking and charging cycles (park-at-work and park-at-home). The driving cycles are collected from the EV trials while the parking and charging cycles are the presumption based on the daily car usage habits. Fig. 6 depicts the diagram of such five-day operational cycle. It is supposed that the EV owner is leaving home and going to their workplace daily at 7:00am, then the driver connects the vehicle to the charger upon arriving at the car park of their office. At the end of the working day at 5:00pm, the owner disconnects the EV from the charger and returns home. Upon arriving home, the owner plugs-in the vehicle to the charger at home. Both parking cycle at home and workplace's car park, the EV battery is kept connected to bi-directional V2G chargers and allowed to participate V2G scenarios to exchange energy with the electrical grid. Fig. 7 shows the details of speed profiles and their SoC variation of ten individual driving cycles within five days operational.

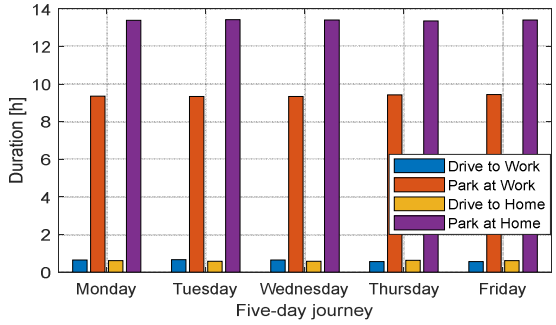

Fig. 6. Five-day operational cycle diagram

To reduce the complexity of the charging process and support the battery ageing evaluation, it is supposed that the charging procedure follows a constant-current (CC) charging principle. The battery will be fully charged from a specific SoC upon arrival (arrival SoC) or after V2G charge (V2G SoC) to the full-charged state. It is noteworthy to set up a minimum discharging SoC for the battery to prevent it from over discharged due to V2G operations, the lower battery SoC discharging limit is set to 50%. This residual energy is also assumed sufficient for an unexpected drive during the parking period.

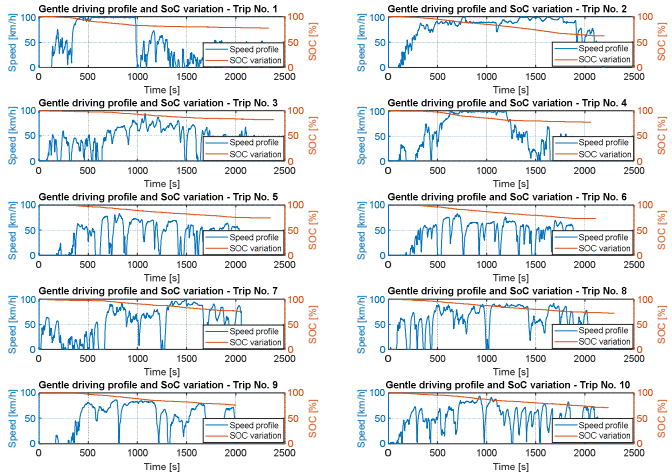

Fig. 7. Detail of ten driving trips of the operational profile

B. Battery Charging Expenditure

Commercial electrical tariff is usually varied depending on off/peak-load periods and date-time of the day/week/month. In this study, one-day electrical regulation cost is selected as shown in Fig. 8 and used as the baseline to estimate the charging fee. This profile is based on the real electrical price reported on Monday 11/10/2021 from the Balancing Mechanism Reporting Service (BMRS) [15], Great Britain. To support the long-term simulation, it is assumed that the selected daily electrical tariff profile is unchanged.

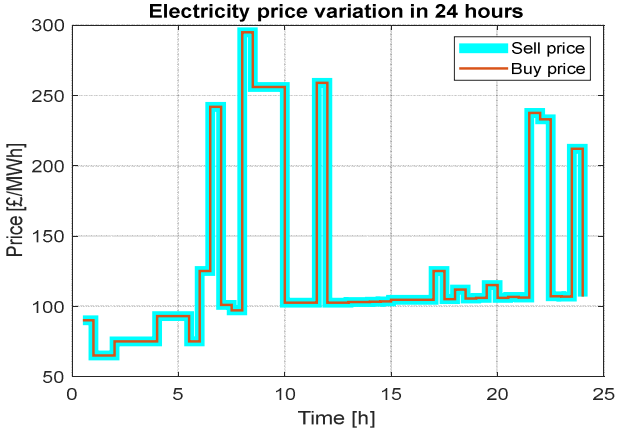

Fig. 8. One day electrical tariff profile (BMRS on 11/10/2021)

C. Charging Strategy Development

The charging scenarios in this section are developed based on a 24kWh 360V battery of an EV while the V2G chargers used at the workplace's car park and at home have the same maximum charge/discharge power of 7kW. In this study, in order to reduce the effect of fast charging to the battery degradation, the chargers can only charge the battery at maximum power at 3.5kW while it can perform discharging the battery at two levels: rapid state at 7kW and slow state at 3.5kW. Hence, three charging strategies are developed to firstly optimise the charging cost and then investigate the influence of charging behaviours to the battery ageing.

1) Standard Charge

Standard charge strategy (STD) is a conventional charging method. The EV battery is fully charged as soon as it is connected to the charger. When the battery is fully charged, it is left in idle state until the next drive.

2) Time-shift Charge

Time-shift charge strategy (TS) is a charging method with a delayed charge time. The battery is in rest state at the point of parking without any charge although it is connected to a charger. The instantaneous SoC at that time is called arrival SoC which presents the SoC upon arrival. Based on the next departure schedule defined by the user, the battery charger is activated automatically at an appropriate time so that the battery is fully charged just before the next driving time.

3) Smart Charge

Smart charge strategy (SC) is developed based on the TS charge principle. It allows the charging process being started when having the lowest total charging cost. The battery is usually in idle state at the arrival SoC while the charge process is delayed until a charging cost is estimated as a smallest one based on the current electrical tariff profile during the entire parking period. In this charging method, both electricity price and next departure's time must be pre-defined so that the charger's controller can calculate a suitable charging start time.

The optimisation function in this charging method is to minimise the charging cost and can be stated as follows:

$$J = \min[\varphi_C] = \min \int_{t=T_C^{ini}}^{T_C^{end}} \varpi_{CHA}(t)\pounds_E(t)dt \quad (9)$$

where, φ_C is the charging cost of each time interval, ϖ_{CHA} is the total charge power to charge the battery from the arrival SoC to 100%SoC, $\pounds_E$ is the electricity price at each time interval, T_C is the time period to charge completely, T_P is the time interval (in this study, T_P equals to 30 minutes).

Fig. 9 presents the time constraint diagram during parking and charging period.

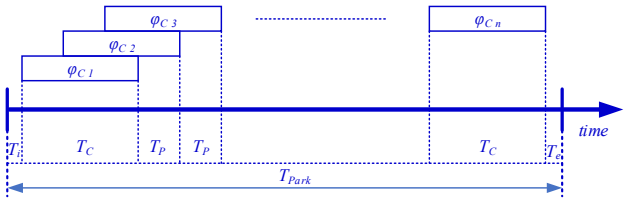

Fig. 9. Parking and charging time constraint

D. V2G Scenarios Development

In this section, a V2G scheme with different discharge C-rates and DoD is evaluated to access the impact of V2G operation on battery degradation. To underpin the development, it is assumed that the battery used for the evaluation is new, thus the initial SoH can be equivalent to 100%. The proposed V2G scheme is developed with two discharging C-rates: high-speed discharge power at 7kW and low-speed discharge power at 3.5kW.

To underpin the evaluation, for each driving trip, the battery will be participated in such V2G scheme with both low and high-speed discharge C-rates upon arrival and connected. As mentioned in the previous section, the minimum discharge SoC is set at 50% which is a safety limit and allows any unexpected drive during parking period. Hence when connected to the charger, if the arrival SoC is higher than the minimum set-point, the battery will be discharged its energy to the minimum set-point or until reaching the charging start time, depending on which condition comes first. Otherwise, the battery does not participate V2G charge.

IV. Simulation Results and Discussions

In this section, simulation of two charging approaches is introduced based on the proposed real-world drive profiles and charging strategies. Without loss of generality, it is assumed that the ambient temperature during both driving and parking periods is stable at 25^0C. The whole simulation evaluation is carried out on a host computer workstation with an Intel Core i7-10850H 2.7GHz CPU, 32GB RAM within Matlab 2021a simulation environment. The sample time of the simulation is fixed at one second.

A. Charge without V2G

The five-day operational profile with three different charging schemes each are presented in Fig. 10. The top subplot shows the current profiles while the bottom one depicts the SoC variation profiles during five days operation. By following their charging principles, STD strategy allows the battery to be charged at the time of connected to the charger. When the battery SoC reaches 100% (fully charged), it turns to resting state until the next drive. On the other hand, TS strategy turns the battery to resting state at the arrival SoC and only allows the battery to be fully charged at a suitable time to ensure its SoC is 100% just before the next drive. Hence, the charging process of both STD and TS strategies disregards the charging cost. In contrary, SC strategy estimates the amount of charging power to fully charge the battery while considers the current electrical tariff profile to solve the optimisation function. Then, an optimal charging cost is determined based on the estimated charging cost of each time interval during the parking period. From here, the charging start time is also defined which allows the battery to be charged with cheapest charging cost.

Fig. 11 illustrates the estimated charging cost of each driving trip using the proposed charging strategies for two operational profiles, respectively. The charging cost of each trip is normalized against the highest one of the fifth trip using STD approach. With the selected electricity tariff profile, the estimated charging costs of the STD approach are higher than those of the TS in most of the cases. In addition, due to disregarding the electricity tariff variation during the charging period, the estimated charging cost of each driving trip using STD and TS approaches are higher than those of the SC strategy, which requires to solve an optimisation function to define an optimal charging start time. The SC approach shows its benefits and capabilities in optimising the charging cost of every charging cycles.

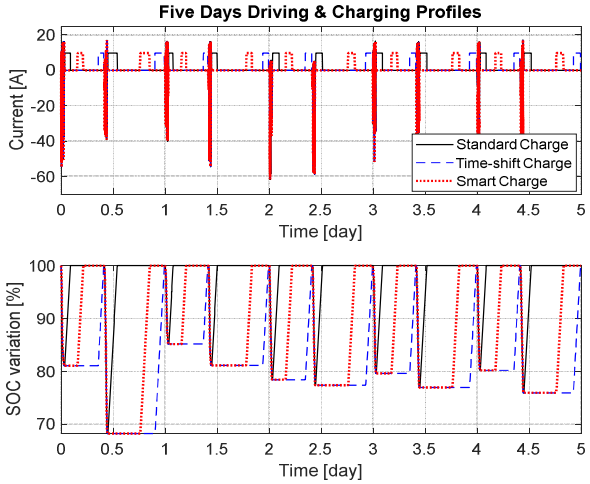

Fig. 10. Five-day operational profile with slow charging rate

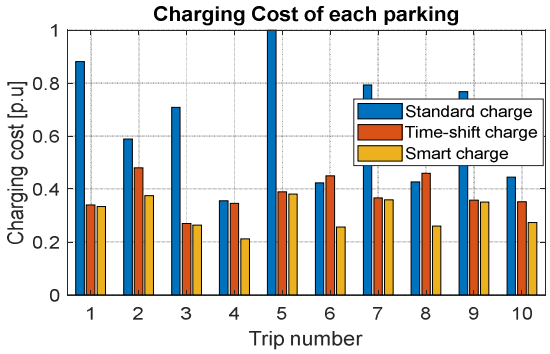

Fig. 11. Estimated charging cost (normalised)

TABLE I
BATTERY AGEING RESULTS

Charge strategy	Rest time (h)	No. of Cycles	Calendar (%)	Cycle (%)	Total (%)
STD	100.04	2.26	0.0176	0.0099	0.0275
TS	100.04	2.26	0.0170	0.0099	0.0269
SC	100.04	2.26	0.0163	0.0099	0.0262

Here, further tests are carried out to further understand the performance of the three charging methods against the battery degradation. Table I depicts the estimated battery ageing in percentage with respect to calendar, cycling and total ageing of such charging strategies. It can be seen that, the rest time and number of cycles of the three charging approaches are exactly the same because these methods do not modify the idle and charge period. Instead, they just vary the resting SoC and the start time of charge. Therefore, the calendar ageing variation is the main contribution to the total degradation while the cycling ageing is less affected by these charging strategies. In term of the battery degradation, the STD charging strategy has higher ageing rate as comparing to the other two because it lets the battery rest at 100% SoC, which may cause faster calendar ageing rate than resting at the arrival SoCs for this battery

chemistry. This behaviour is consistent with the ageing behaviour described in Fig. 1. The SC strategy seems having higher benefit than the other two because it causes less ageing for the first five days operation. Furthermore, in term of the charging cost optimisation, both TS and SC charge approaches bring higher profits while still satisfy the charging requirements.

B. *Charge with V2G*

Based on the results from the previous section, the SC strategy demonstrates the superlative in both optimising the charging cost and lowering the total ageing of the battery. This section evaluates the ageing behaviours of the battery under such charging strategy when attending low-speed and high-speed V2G scenarios. V2G-L and V2G-H terms represent the low- and high-speed V2G scenarios, respectively. As discussed, the maximum battery discharge power for low-speed V2G is 3.5kW while that for the high-speed V2G is 7kW.

Because the arrival SoCs of all trips of this profile are higher than the minimum SoC safety limit, which is set to 50%SoC, the battery will thus participate in V2G operations upon arrival and connected. The battery will be discharged to 50% SoC or until reaching the charging start time, whichever comes first. Fig. 12 shows the current and SoC variation of the five-day operational driving profile when participating in the two V2G scenarios during parking period.

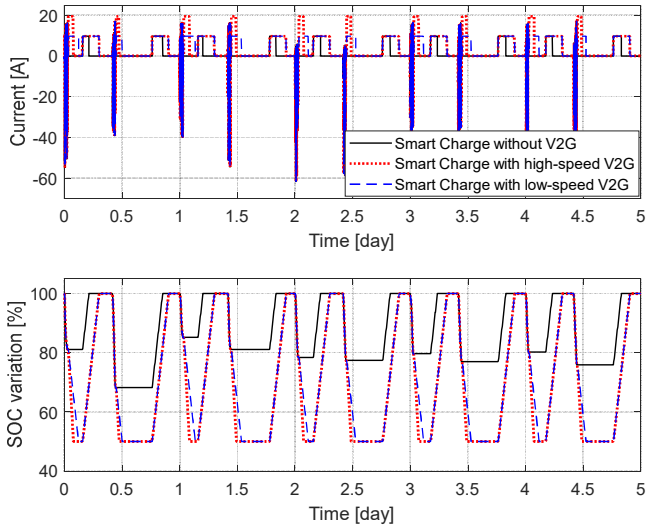

Fig. 12. Five-day operational profile with low- and high-speed V2G

Based on the SoC profile in bottom subplot, the battery under the smart charge with low- and high-speed V2Gs have exchanged the energy with the grid by firstly discharging its energy to 50% SoC right after connected to the charger upon arrival; and then when reaching the optimal charging cost or pre-calculated charging start time, the battery is fully charged. This task may help to support the grid in term of supplement the energy for further V2G missions such as frequency regulation or peak load balancing. Furthermore, although the same amount of energy is sent and received after each V2G scenario, there are potential benefits if we a right strategy based on the difference between the charge and discharge costs.

Table II presents the summary of battery degradation behaviours after participating in such two V2G scenarios for the first five days operation. Both scenarios reduce the idle time of the battery significantly, which help to notably reduce the calendar ageing from 72 – 80% comparing to those of the SC without V2G. However, these scenarios cause arising the charge throughput 2.26 times, which inflates the cycling ageing from 7.67 – 8.3 times. Hence, the total ageing increases from 3 – 3.3 times as comparing to the baseline SC strategy.

TABLE II
BATTERY AGEING RESULTS

Charge strategy	Rest time (h)	No. of Cycles	Calendar (%)	Cycle (%)	Total (%)
SC	100.04	2.26	0.0163	0.0099	0.0262
V2G-L	61.06	5.10	0.0032	0.0759	0.0791
V2G-H	70.8	5.10	0.0046	0.0823	0.0869

Fig. 13. Five-day operational profile with low and high-speed V2G

Besides, Fig. 12 also implies that the two V2G scenarios have the same energy throughput although attending to two different V2G strategies. The only difference is the discharge rate when discharging the energy from the battery to the grid. This discharging scheme helps to evaluate the impact of V2G speed to the cycling ageing behaviour of the battery. From Table II, the number of cycles of the low- and high-speed V2G scenarios are the same, but due to the discharge rate is much different, the cycle ageing of the later is also higher than that of the former up to 8% after five days operation.

V. CONCLUSION

A. *Conclusion*

This study evaluated the degradation behaviour of the EV battery during charging under different charging strategies with and without participating in the V2G scenarios. The developed battery ageing model has successfully predicted the ageing behaviour of the battery under various operational condition of real-world energy driver profiles. The simulation results demonstrated that the EV battery can be employed in V2G operations with emphatically advantages. However, it is necessary to carefully consider the trade-off between the benefits and the battery degradation costs. A further optimisation problem should be proposed with respect to specific cases to determine whether having smart charge V2G and overcome the limitation of the study. Hence, further works are required to fully understand the degradation behaviours of the battery, especially for long-term operation.

B. *Future Works*

Four tasks are required to underpin the study as follows:

- Training dataset should be carried out at different temperatures to represent the complete operational conditions of the battery in real applications.
- Charging rate should be considered to evaluate the impact of charging current versus charging time. This is useful to evaluate the effect of calendar ageing as fast charging will increase the idle state after the charge.
- Long-term verification is required to fully understand the degradation behaviour of the battery under different charging strategies.
- Transferability of the developed degradation model and charging strategies to other battery chemistries and form formats.

ACKNOWLEDGMENT

This research was supported by Innovate UK via EV-elocity (project no. 104250) and TE1 (project no. 28186).

REFERENCES

[1] M. Petit, E. Prada, and V. Sauvant-Moynot, "Development of an empirical aging model for Li-ion batteries and application to assess the impact of Vehicle-to-Grid strategies on battery lifetime," *Applied Energy,* vol. 172, pp. 398-407, 2016/06/15/ 2016, doi: https://doi.org/10.1016/j.apenergy.2016.03.119.

[2] A. Ahmadian, M. Sedghi, A. Elkamel, M. Fowler, and M. Aliakbar Golkar, "Plug-in electric vehicle batteries degradation modeling for smart grid studies: Review, assessment and conceptual framework," *Renewable and Sustainable Energy Reviews,* vol. 81, pp. 2609-2624, 2018/01/01/ 2018, doi: https://doi.org/10.1016/j.rser.2017.06.067.

[3] O. Kolawole and I. Al-Anbagi, "Electric Vehicles Battery Wear Cost Optimization for Frequency Regulation Support," *IEEE Access,* vol. 7, pp. 130388-130398, 2019, doi: 10.1109/ACCESS.2019.2930233.

[4] T. M. N. Bui, T. Q. Dinh, J. Marco, and C. Watts, "Development and Real-Time Performance Evaluation of Energy Management Strategy for a Dynamic Positioning Hybrid Electric Marine Vessel," *Electronics,* vol. 10, no. 11, 2021, doi: 10.3390/electronics10111280.

[5] N. I. Nimalsiri, C. P. Mediwaththe, E. L. Ratnam, M. Shaw, D. B. Smith, and S. K. Halgamuge, "A Survey of Algorithms for Distributed Charging Control of Electric Vehicles in Smart Grid," *IEEE Transactions on Intelligent Transportation Systems,* pp. 1-19, 2019, doi: 10.1109/TITS.2019.2943620.

[6] U. R. Koleti, T. N. M. Bui, T. Q. Dinh, and J. Marco, "The Development of Optimal Charging Protocols for Lithium-Ion Batteries to Reduce Lithium Plating," *Journal of Energy Storage,* vol. 39, p. 102573, 2021/07/01/ 2021, doi: https://doi.org/10.1016/j.est.2021.102573.

[7] S. Amamra and J. Marco, "Vehicle-to-Grid Aggregator to Support Power Grid and Reduce Electric Vehicle Charging Cost," *IEEE Access,* vol. 7, pp. 178528-178538, 2019, doi: 10.1109/ACCESS.2019.2958664.

[8] T. M. N. Bui, M. Sheikh, T. Q. Dinh, A. Gupta, D. W. Widanalage, and J. Marco, "A Study of Reduced Battery Degradation through State-of-Charge Pre-Conditioning for Vehicle-to-Grid Operations," *IEEE Access,* pp. 1-1, 2021, doi: 10.1109/ACCESS.2021.3128774.

[9] M. F. Niri, T. M. N. Bui, T. Q. Dinh, E. Hosseinzadeh, T. F. Yu, and J. Marco, "Remaining energy estimation for lithium-ion batteries via Gaussian mixture and Markov models for future load prediction," *Journal of Energy Storage,* vol. 28, p. 101271, 2020/04/01/ 2020, doi: https://doi.org/10.1016/j.est.2020.101271.

[10] T. M. Bui, M. Faraji-Niri, D. Worwood, T. Q. Dinh, and J. Marco, "An Advanced Hardware-in-the-loop Battery Simulation Platform for the Experimental Testing of Battery Management System," presented at the 23rd International Conference on Mechatronics Technology Salerno, Italy, 2019.

[11] C. Pastor-Fernández, T. F. Yu, W. D. Widanage, and J. Marco, "Critical review of non-invasive diagnosis techniques for quantification of degradation modes in lithium-ion batteries," *Renewable and Sustainable Energy Reviews,* vol. 109, pp. 138-159, 2019/07/01/ 2019, doi: https://doi.org/10.1016/j.rser.2019.03.060.

[12] Y. Li *et al.*, "Data-driven health estimation and lifetime prediction of lithium-ion batteries: A review," *Renewable and Sustainable Energy Reviews,* vol. 113, p. 109254, 2019/10/01/ 2019, doi: https://doi.org/10.1016/j.rser.2019.109254.

[13] J. de Hoog *et al.*, "Combined cycling and calendar capacity fade modeling of a Nickel-Manganese-Cobalt Oxide Cell with real-life profile validation," *Applied Energy,* vol. 200, pp. 47-61, 2017/08/15/ 2017, doi: https://doi.org/10.1016/j.apenergy.2017.05.018.

[14] E. Redondo-Iglesias, P. Venet, and S. Pelissier, "Calendar and cycling ageing combination of batteries in electric vehicles," *Microelectronics Reliability,* vol. 88-90, pp. 1212-1215, 2018/09/01/ 2018, doi: https://doi.org/10.1016/j.microrel.2018.06.113.

[15] BMRS. "Electricity Data Summary." Balancing Mechanism Reporting Service. https://www.bmreports.com/bmrs/?q=eds/main (accessed 1st November, 2021).